Design and Alignment of an All-Spherical Unobscured, Four-Mirror Image Relay for an Ultra-Broadband Subpetawatt Laser

E. M. Schiesser,[1,2] S.-W. Bahk,[1] J. Bromage,[1,2] and J. P. Rolland[2]

[1]Laboratory for Laser Energetics, University of Rochester
[2]Institute of Optics, University of Rochester

LLE is developing an ultra-broadband optical parametric chirped-pulse–amplified laser system.[1] This laser, the Multi-Terawatt Optical Parametric Amplifier Line (MTW-OPAL),[2] is designed to produce 7.5-J, 15-fs pulses with a 200-nm bandwidth from 810 nm to 1010 nm through multiple stages of noncollinear optical parametric amplifiers (NOPA's). Image relays between NOPA's preserve the beam quality and sequentially magnify the beam size according to its amplified energy level to keep the maximum fluence below the damage threshold. The final relay after the last NOPA stage (referred to as NOPA5 since it is the fifth amplifier) requires an all-reflective, unobscured optical relay to avoid introducing additional longitudinal chromatic aberration, also known as radial group delay (RGD).[3–5] RGD refers to the fact that refractive image relays delay the pulse in the center of the beam with respect to the pulse in the outer edge of the beam as the center beam goes through thicker material in the lens. This RGD is of the order of hundreds of femtoseconds so it is significantly larger than the ideal 15-fs design pulse width and would greatly reduce the focused intensity. The final all-reflective image relay, also referred to as an achromatic image relay (AIR), removes the longitudinal chromatic aberrations and RGD by avoiding lenses in favor of using mirrors. The AIR for NOPA5 performs two roles: it acts as a beam expander to create a 90 × 90-mm beam from the 45 × 45-mm output from NOPA5, and it relays the NOPA5 (N5) output to the fourth grating (G4) in the grating compressor chamber (GCC). These two roles must be achieved simultaneously; consequently, two sets of conjugate planes must be simultaneously realized: the "far-field" (FF) collimation planes and the "near-field" (NF) pupil imaging planes. This simultaneous dual-conjugate imaging case has been investigated for two refractive elements and four refractive elements by Wang *et al.*[6]

In optical design, there is often a trade-off between complexity and performance. Off-axis conic sections are the most obvious choice for unobscured, small-FOV (field-of-view) designs like the AIR, as we have previously reported.[7] However, it is important to understand if we can achieve our goals with simpler spherical optics since this reduces complexity and therefore the cost. Instead of field-bias or aperture offset as in an off-axis conic design, one can tilt the optical components to avoid obscuration. Buchroeder[8,9] details many examples of tilted component telescopes, some of which have only spherical components. These designs use tilted components to avoid obscuration, but the relative tilts must be chosen to balance the resulting aberrations. Steven and Dubra[10] describe the design of a two-mirror relay using tilted spherical components.

The design detailed in the present work is a four-mirror all-spherical design that tilts the mirrors to avoid obscuration. We show the theoretical basis for the correction of field-constant coma and field-constant astigmatism using two of the mirror tilts. We then show the alignment of the design in a test-bed setup.

There are nine first-order parameters for this four-mirror system: the input and output working distances, the three distances between the mirrors, and the four radii of curvature of each mirror. The magnification constraint, NF imaging requirement, and FF collimation requirement determine three of these variables. The other six variables are available to meet the layout and space requirements. To meet those requirements, the five distances are specified within a certain range based on the space constraints in the GCC, leaving only one truly free variable: the curvature of the first mirror. This variable is constrained by the stay-out zone created by the damage threshold of the mirrors, which constrains the size of the beam on the mirrors.

With the first-order parameters determined, the next step was to create an unobscured configuration. To do so, we can tilt the components appropriately; however, tilting spherical components results in aberrations. Buchroeder showed that these types of designs, known as tilted-component telescopes, can correct the aberrations caused by the tilts by appropriately tuning the tilts of the mirrors.[8,11] In addition, Rogers showed the same using the nodal aberration theory (NAT) for two and three mirrors for extended fields of view.[12] Because the FOV for the AIR is small at 0.14°, we can achieve the required correction while maintaining enough freedom in the design to keep the AIR within the space constraints of the GCC.

Given the minimum tilt angle of M1 required to remove the obscuration of M2, we can use the theoretical framework of NAT to predict the M3 and M4 tilts necessary to correct the field-constant astigmatism and field-constant coma induced from the tilts of M1 and M2. The system of equations involves two NAT aberration terms composed in terms of the sigma vectors of each surface. The sigma vectors are then related to the tilts of each surface. Because of the quadratic dependence of field-constant astigmatism on the sigma vector, there are two solutions; however, only one solution is unobscured, shown in Fig. 1. The angles from the theoretical analysis were ultimately optimized to balance the aberrations and reduce the overall rms wavefront error.

Figure 1
The final layout of the AIR mirrors, showing the ray path from the central field point.

An alignment plan for the AIR has been developed and tested. The alignment procedure consists of two stages: course alignment and fine alignment. The course alignment stage uses the arm of a precision coordinate-measuring machine (CMM) to place precision-machined pinhole jigs. The CMM arm is a FARO Gage Plus, from which we achieved of the order of 100-μm placement accuracy of the pinholes.[13] Passing a pencil beam from an alignment laser diode through the pinholes establishes a line that serves as the optical axis. Since the mirrors are spherical, guiding the pencil beam through the pinholes using tip/tilt and z travel on each mirror can be used to position the center of curvature close to the nominally designed position. All four mirrors can be coarsely aligned sequentially with this method. Tolerance analysis assuming 100-μm accuracy in the mirror placement of the AIR design shows that the coarse alignment using the pinholes is adequate to position the mirrors accurately enough such that fine alignment of M4 tip, tilt, and defocus can correct any residual defocus and astigmatism still present after course alignment. Additionally, M3 tip/tilt can be used to correct residual coma, if necessary.

To test the feasibility of the alignment plan and to troubleshoot possible difficulties before the final alignment in the GCC, we developed a test bed to replicate the *in-situ* alignment before the final system is aligned at LLE. The essential components of the test bed are a 532-nm laser diode, a custom wavefront sensor,[14] a polarizing beam splitter, a beam expander, and several planar mirrors.

The NOPA5 crystal outputs a 45 × 45-mm collimated beam. To replicate this in the test bed, we use two beam expanders as shown in Fig. 2: The first is a 4× beam expander that focuses the output of a laser diode into a 25-μm pinhole used as a spatial filter. The resulting Gaussian beam is then collimated and truncated using a square apodizer before passing through a polarizing beam splitter (PBS). The second beam expander then enlarges the beam to 45 × 45 mm. A quarter-wave plate at the focus of the 10× beam expander rotates the polarization of the return beam from vertical to horizontal to reduce spurious reflections from PBS. Additionally, an adjustable iris is used to create a pencil beam for the course alignment step. The return beam reflects off the PBS interface to a wavefront sensor and a blank mirror substrate with a wedge acting as a second beam splitter. The second return beam is directed into a focusing lens and charge-coupled–device camera used to maintain alignment.

The subsequent wavefront after the course alignment routine using the pinholes is shown in Fig. 3(a). The dominant aberration in the wavefront after the course alignment step appears to be defocused. Figure 4 shows the peak-to-valley (p–v) and rms

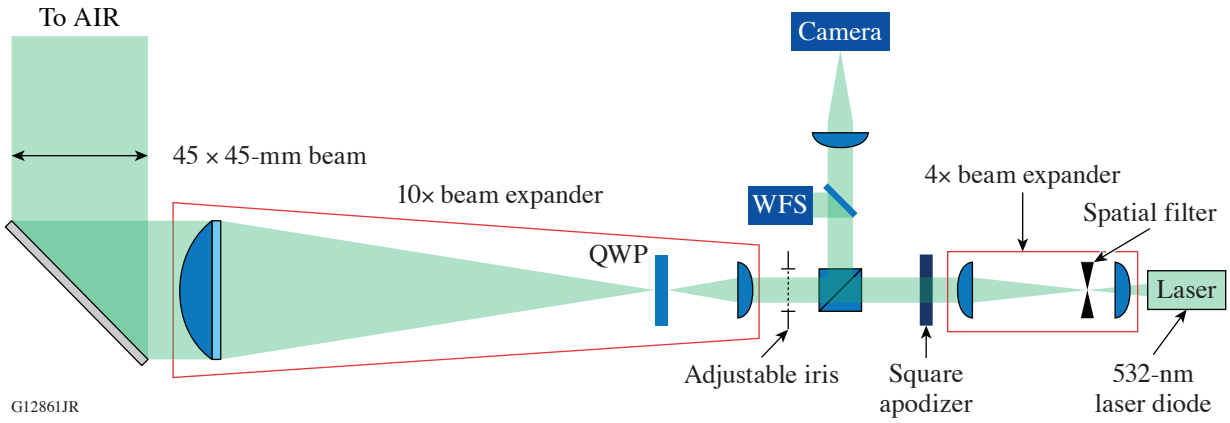

Figure 2
The test-bed components to produce a 45 × 45-mm beam and to measure the return wavefront. QWP: quarter-wave plate; WFS: wavefront sensor.

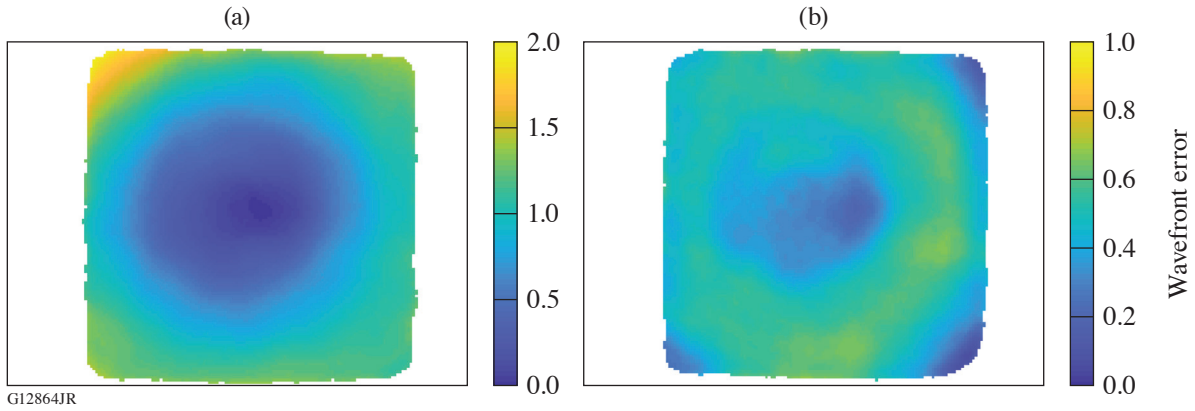

Figure 3
The double-pass wavefront given in waves at 532 nm for (a) after the course alignment step and (b) after the fine alignment steps. Note that the color scale ranges from [0,2] waves for (a) and from [0,1] waves for (b).

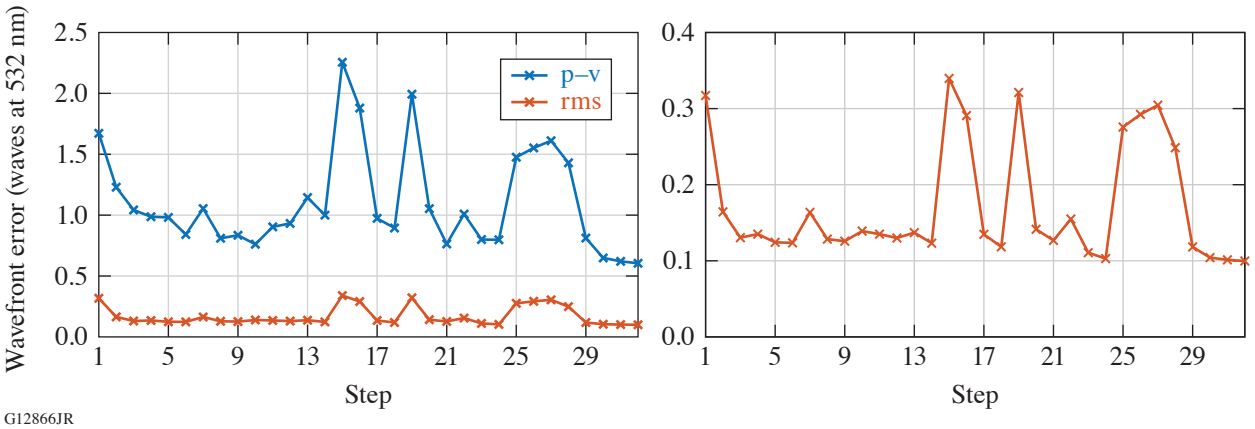

Figure 4
(a) The p–v and rms values of the wavefront at each step; (b) the rms WFE values of the wavefront at each step.

wavefront error (WFE) of the wavefront at each step in the fine alignment process. This defocus was more than predicted by the tolerances of the CMM coarse alignment stage—a clue to another issue that will be addressed later.

Figure 3(b) shows the measured wavefront error after fine alignment. There is residual spherical aberration, as predicted by the ray-tracing model. Additionally, there is still some coma (Z7/8) present and higher-order modes are also becoming dominant. Since we reached the desired p–v and rms WFE targets, however, we stopped the alignment process. With the aid of the program used to decompose the wavefront and predict the adjustments, the fine alignment routine can be completed in less than 1 h. After completing fine alignment, the resulting wavefront p–v at 532 nm was 0.61 waves and the rms WFE was 0.10 waves in double pass. Applying the reduction factor of 3.42 to the measured wavefronts in Fig. 3, we have 0.176 waves p–v and 0.029 waves rms. Therefore, we can expect a wavefront p–v of less than 0.2 waves and rms WFE of less than 0.05 waves at 910 nm at the output of the AIR using this method.

After the wavefront was aligned, the magnification of the beam was measured. Minimizing magnification error is important for laser systems with large beams. For the AIR, the magnification was required to be –2.00±2%. To measure the magnification in the test bed, a mask with holes was placed at the object plane and the distance between the images of the holes was measured in the image. The relative distance between the holes was measured.

The result was a magnification of –2.13±2%, which is a +7.5% change from the required value of –2.00±2%. At first, this error was suspected to be caused by uncertainties in the alignment process. However, the course and fine alignment processes were repeated multiple times to test this suspicion, and the magnification was remeasured each time. The measured value of the magnification varied by less than 1% between alignments. To bring the magnification back into spec, the position of another mirror besides M4 must be adjusted; however, the same space constraints in the design process also restrict us here: M2 is already very close to the GCC wall. Although there is some room to move M1, moving it would require changing the input angle of the beam from N5, which is not ideal. M3, being the only mirror left, is the best candidate to move. To test how far was required, the location of M3 was moved by 75 mm toward M2 to shorten the focal length of the M3/M4 pair in the model with the measured radii, which reduced the magnification by 3.5%. This adjustment reduced the output working distance to the image plane (G4) by 75 mm. This change was reproduced in the test bed, and the magnification was remeasured to be 2.07, bringing the magnification error down from 7.5% to 3.5%. Based on the model, to bring the magnification error down another 3.5%, we could move the M3 mirror by another 75 mm. Since the test-bed optics likely do not have exactly the same radii as the *in-situ* AIR optics, this final M3 mirror adjustment was not performed on the test bed. The actual compensation will be based on the measurements of the *in-situ* AIR mirrors.

The design of an unobscured reflective laser relay comprising four tilted spherical mirrors has been described. We showed the theoretical basis for such a four-mirror design using first-order optical matrix methods and NAT. We then described the process of aligning the design in a test bed to demonstrate an effective alignment method for such a design. We were able to achieve a nominal design that met our specifications and also successfully align the design in a test-bed environment to achieve our target wavefront error of less than 0.25 waves p–v and 0.07 waves rms.

This material is based upon work supported by the Department of Energy National Nuclear Security Administration under Award Number DE-NA0003856, the University of Rochester, and the New York State Energy Research and Development Authority.

1. S.-W. Bahk, J. Bromage, and J. D. Zuegel, Opt. Lett. **39**, 1081 (2014).
2. J. Bromage *et al*., High Power Laser Sci. Eng. **7**, e4 (2019).
3. Z. Bor, Opt. Lett. **14**, 119 (1989).
4. Zs. Bor and Z. L. Horváth, Opt. Commun. **94**, 249 (1992).
5. H.-M. Heuck *et al*., Appl. Phys. B **84**, 421 (2006).
6. D. Y. Wang, D. M. Aikens, and R. E. English, Jr., Opt. Eng. **39**, 1788 (2000).

7. E. M. Schiesser *et al*., Opt. Lett. **43**, 4855 (2018).

8. R. A. Buchroeder, Appl. Opt. **9**, 2169 (1970).

9. R. A. Buchroeder, Optical Sciences Center, University of Arizona, Tucson, AZ, Optical Sciences Technical Report 68 (1971).

10. S. Steven, J. Bentley, and A. Dubra, Opt. Express **27**, 11205 (2019).

11. R. A. Buchroeder, "Titled Component Optical Systems," Ph.D. thesis, University of Arizona, 1976.

12. J. R. Rogers, Opt. Eng. **39**, 1776 (2000).

13. FARO Gage & Gage-PLUS, 20 February 2009, http://www.dirdim.com/pdfs/DDI_FARO_Gage.pdf.

14. S.-W. Bahk and C. Dorrer, in *Imaging and Applied Optics*, OSA Technical Digest (online) (Optical Society of America, Washington, DC, 2013), Paper CM3C.4.